 SL, vol.3, no.1, pp.59-86, 2010

Interaction Multiple Interacting and Coalescing Semi-Elliptical Surface Cracks in Fatigue-Part II: Experimental Study

S. K. Patel[1], B. Dattaguru[2] and K. Ramachandra[3]

Abstract: A crack growth model for multiple surface cracks has been proposed and used in the study of multiple interacting and coalescing semi-elliptical cracks. Using this crack growth model the effect of multi-site damage on residual life is studied in detail. The stress intensity factor, crack shape development and crack propagation life are discussed. Numerical predictions of crack propagation lives have been verified by an experiment crack growth study on specimens having coplanar multiple semi-elliptical cracks made of an aero-engine disk material. The crack shape evolution and life estimated from numerical methods are found to be in good agreement with the experimental results.

1 Introduction

The categories of the flaws normally assumed to be present in the bladed-disk assembly of gas turbine engine at "hot spots" are shown in Fig. 1. Broadly three categories of flaws can be assumed in the assembly: (1) Single flaw such as semi-elliptical/corner/circular (2)Multiple interacting flaws (3) Multi-element flaws: for example effect of flaw in a blade on flaw in a disk.

In this work, second category of cracks has been considered for further study. The fatigue crack growth of multiple semi-elliptical surface cracks in the fundamental mode of fracture has been studied experimentally and numerically.

Mainly three approaches are available for assessment of multiple surface cracks in fatigue viz. ASME XI code [ASTM E740 (1987)] (Rules for in-service inspection of nuclear power plant components, 1977), BSI PD6493 code[BSI PD6493 (1980)] (Guidance for the derivation of acceptance levels for defects in fusion welded joints, 1980) and NIIT ('No interaction and immediate transition'). As per ASME XI

[1] Gas Turbine Research Establishment, Bangalore
[2] Department of Aerospace Engineering, Jain University, Bangalore (formerly at) Indian Institute of Science, Bangalore
[3] Formerly at Gas Turbine Research Establishment, Bangalore

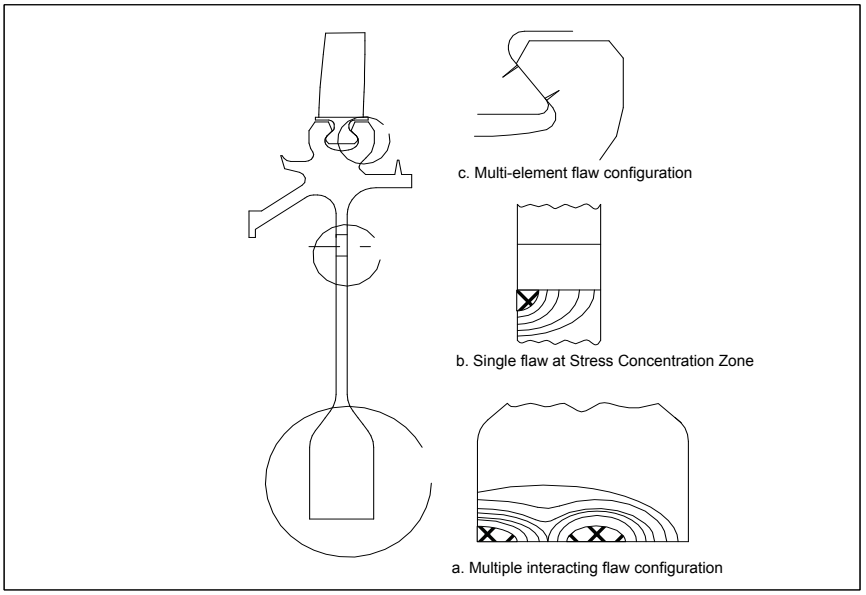

Figure 1: Schematic of initial flaws in the compressor bladed-disk assembly

and BSI PD6493 codes, the adjacent cracks should be re-characterized to a single crack if certain geometric conditions are satisfied. Clearly, this method excludes the stages of interaction and coalescence.

The NIIT method assumes no interaction between the cracks before the inner tips of the cracks touch and immediate formation to a single elliptical shaped crack after they touch. This actually means that the advance of each adjacent crack is individually computed until they come together, and the region of coalescence cracks is neglected. Some experimental investigations into fatigue growth of coalescing cracks (Soboyejo et al.[Soboyejo, Knott, Walse and Cropper (1990)], Iida [Iida (1983)], Grandt [Grandt Jr. (1986)], McComb et al.[McComb, Pope and Grandt Jr. (1986)], Soboyejo et al.[Soboyejo, Kishimoto, Smith, and Knott (1989)], To et al.[To, Lambert and Burns (1993)]) have been made, indicating that NIIT can make better predictions of fatigue lives than that suggested by both the ASME XI and BSI PD6493 codes. Another alternate approach could be based on step-by-step three-dimensional Finite Element method. Although, this approach is powerful enough to simulate the fatigue crack growth of multiple surface cracks, the cost and running time could be enormous. Here, a simplified semi-analytical/numerical approach is presented to simulate the growth of multiple surface cracks in fatigue considering interaction and coalescence of cracks.

Song et al [Song, Shen and Shieh (2002)] used a parameter based on Sih's energy approach to predict semi-elliptical crack growth and they conducted experimental investigations on 2024-T4 aluminum alloy specimens as per ASTM standard. Their method of measuring the crack growth was to break open several specimens tested to different stages and measure crack growth from the fracture surface. They had good comparison between the predicted and measured crack growth. Nilsson et al [Nilsson, Harisson and Mansson (2004)] conducted experimental study on the growth behavior at the deepest point of a semi-circular flaw in Inconnel 718 material. They measured crack closure and used it to correct crack growth rates and were able to show excellent correlations. Song and Shieh [Song and Sheih (2004)] made compliance measurements of crack closure at the depth and surface points using back face and near tip gauge. They conducted experiments on AISI alloy steel under constant and variable amplitude loading. The crack shape development based on closure measurements agreed very well with predicted shapes. However, these measurements are easily possible in case of single crack and not possible for the case of multiple cracks merging and not attempted in the current work.

In the current work, the surface crack specimens of aero-engine disk material Inconel-718 are tested under uni-axial fatigue loading. Crack shape development has been investigated in detail. This is a comprehensive study combining both interacting and coalescing phases starting with two cracks in the close neighborhood and taking them through the stage of merging into a single crack. These experimental observations are used in evaluating the numerical tools developed in this work for fatigue crack growth simulation.

Three degrees of freedom model is proposed in the present work to study the fatigue crack growth of twin coplanar semi-elliptical cracks. The interaction effects are included through the use of interaction factors as obtained in part-I (Patel et al. [Patel, Dattaguru, Ramachandra(2011)]). The interaction factors are fitted by polynomial equations to facilitate their direct use in the three degrees of freedom model. The results are compared with experimental study on multiple cracks.

In safety critical aerospace and thick piping structures this work is significant in predicting the remaining life of aged components with multi-site damage.

2 Fatigue Crack Growth Model for Multiple Surface Cracks

As mentioned before the NIIT method assumes no interaction before the inner tips of the cracks touch and immediate formation to a single elliptical shaped crack after they touch. This actually means that the advance of each adjacent crack is individually computed until they come together, and the region of coalescence cracks is neglected. Here, a simplified semi-analytical/numerical approach is presented to

simulate the growth of multiple surface cracks in fatigue considering interaction and coalescence of cracks. The growth of multiple surface cracks in fatigue can be divided in various phases as follows:

- Multiple cracks without interaction
- Multiple cracks with interaction
- Coalescing cracks
- Formation and growth of a single crack

Three degrees of freedom per crack is thought to be appropriate for simulation of multiple surface cracks in fatigue as shown in Fig. 2. For clarity, the procedure is explained with respect to symmetric cracks where it is sufficient to consider one crack in simulation. Similar procedure can be applied to all the cracks in case of un-symmetric crack configuration. Assumptions applicable to the three degree of freedom model as proposed here are listed below:

1. The fatigue crack will grow in a semi-elliptical shape.
2. Crack growth rate at the ends of the semi-elliptical crack will be assumed to be dependent on the value of the local SIF only.
3. The material is assumed to be homogeneous and isotropic.
4. Paris crack-growth equation is assumed to be valid.

The crack extension is assumed to be in normal direction at the considered location. Until the interaction (phase-I) the simulation procedure is same as for single surface crack and the stress intensity factor for a single crack is assumed to be applicable. Once the cracks come in close vicinity, they start interacting. Here, the interaction effects are considered by multiplying the stress intensity factor of single crack with interaction factor. It is common practice to assume that the interaction effect is important at location B only and its effect is considered negligible on points A and C. Similar procedure to account the effect of interaction was proposed by Grandt [Grandt Jr. (1986)] and Soboyejo et al.[Soboyejo, Kishimoto, Smith, and Knott (1989)]. Here, a modified procedure for crack extension during the interaction phase is proposed although in principal it is same as proposed earlier [Grandt Jr. (1986), Soboyejo, Kishimoto, Smith, and Knott (1989)]. In references [Grandt Jr. (1986), Soboyejo, Kishimoto, Smith, and Knott (1989)] the crack extensions at locations A, B and C are assumed to occur in normal direction based on the stress intensity factors and Paris equation. But once the crack extensions occur at these

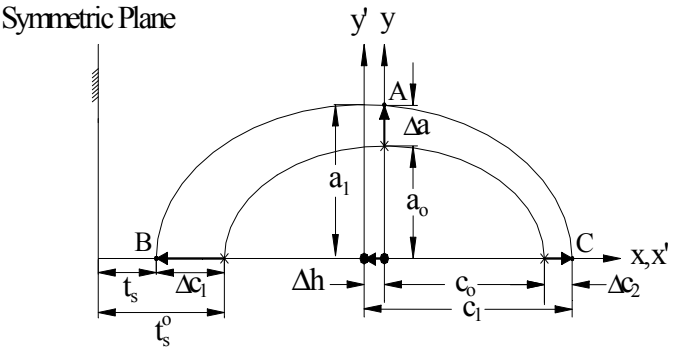

Figure 2: Semi-elliptical interacting surface cracks before and after crack extension (only symmetric crack is shown)

three locations, the ellipse (semi-ellipse) can not remain ellipse since the extension at locations A and C would be different due to interaction effects. This can be avoided if the center of ellipse is shifted. This is also logical, because as cracks grow and form a single crack, its center would be shifted. Thus during interaction, if a_0 and c_0 represent the crack geometry at current step and a_1 and c_1 represent the geometry of the crack after the fatigue crack growth increments at A, B and C as shown in Fig. 2, then it can be written as

$$c_1 = c_0 + \frac{1}{2}(\Delta c_1 + \Delta c_2) \tag{1}$$

$$a_1 = \frac{(a_0 + \Delta a)}{\sqrt{1 - \frac{\Delta h^2}{c_1^2}}} \tag{2}$$

Where $\Delta h = c_0 + \Delta c_2 - c_1$.

The interspacing could be updated as follows

$$t_s = t_s^0 - \Delta c_1$$

Where t_s^0 and t_s are spacing between cracks at 'y' equal to zero before and after crack extension respectively and Δa_1, Δc_1 and Δc_2 are crack extensions at locations A, B and C respectively. Note that Δh is negative in the above equations.

Once the cracks approximately touch each other, coalesce phase begins. The interaction factor defined by eq. (5)-(6) (Patel et al. [Patel, Dattaguru, Ramachandra(2011)]) is not defined at $\bar{t}_s = 0$, therefore it is always avoided in crack growth

simulation of multiple cracks. During coalesce the third degree of freedom is taken at coalesce plane i.e. at location 'B' as shown in Fig. 3 and direction of extension is taken along the coalesce plane which is also bi-normal to crack fronts at point 'B'.

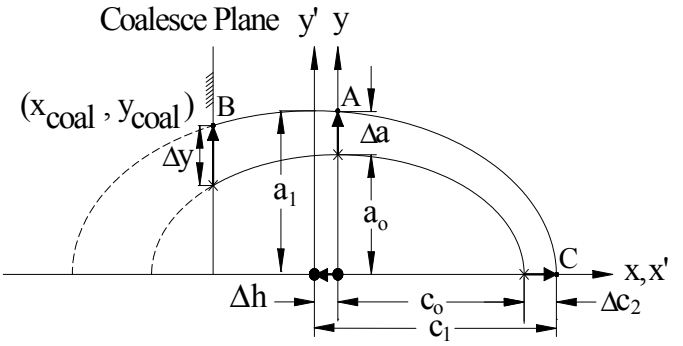

Figure 3: Semi-elliptical coalescing surface cracks before and after crack extension (only symmetric crack is shown)

The updated geometry after crack extension can be obtained using the generalised equation for ellipse having shifted center point by 'Δh' in coordinate system 'xy', the corresponding equations at points A, B and C can be written as

$$\frac{(x_{coal}-\Delta h)^2}{c_1^2}+\frac{y_{coal}^2}{a_1^2}=1 \tag{3a}$$

$$\frac{\Delta h^2}{c_1^2}+\frac{(a_0+\Delta a)^2}{a_1^2}=1 \tag{3b}$$

$$\frac{(c_0+\Delta c_2-\Delta h)^2}{c_1^2}=1 \tag{3c}$$

Using eqs.(3a-b) , an equation in terms of c_1 can be written as

$$y_{coal}^2\left(c_1^2-\Delta h^2\right)=(a_0+\Delta a)^2\left\{c_1^2-(x_{coal}-\Delta h)^2\right\} \tag{4}$$

By substituting $\Delta h = c + \Delta c_2 - c_1$ in eq.(4) from eq.(3c) and solving for c_1, we get

$$c_1 = \frac{-(a_0+\Delta a)^2 (x_{coal} - c_0 - \Delta c_2)^2 + (c_0+\Delta c_2)^2 y_{coal}^2}{2(c_0+\Delta c_2) y_{coal}^2 + 2(x_{coal} - c_0 - \Delta c_2)(a_0+\Delta a)^2} \tag{5}$$

and by replacing c_1 in eq.(3b), a_1 can be written as

$$a_1 = \frac{(a_0+\Delta a)}{\sqrt{1 - \frac{\Delta h^2}{c_1^2}}} \tag{6}$$

During coalesce, the crack extensions Δc, Δa, Δy at locations A, B and C respectively are predicted using stress intensity factor and Paris equation. The stress intensity factor at B is multiplied by interaction factor (4), Part-I (Patel et al. [Patel, Dattaguru, Ramachandra(2011)]). Using Δc, Δa and Δy, new crack dimensions are predicted. X_{coal} and Y_{coal} are updated as X_{coal} =X_{coal} + Δh and Y_{coal} =Y_{coal} + Δy respectively.

The coalescence phase is assumed to be completed when Y_{coal} reaches 99% of a_1 and the length of the single crack would be c+X_{coal}. Subsequently, the crack growth follows the procedure same as that for a single crack. In all the following simulations of multiple cracks Δa is taken equal to 0.0001 times of 'a_o'.

3 Empirical Equation for Interaction Factor for Multiple Semi-Elliptical Cracks

The interaction factors were obtained in part-I (Patel et al. [Patel, Dattaguru, Ramachandra(2011)]) for a wide range of parameters of twin semi-elliptical cracks. In order to use the multi-degrees of freedom model for crack propagation, an empirical equation for the interaction factor was obtained in Part-I. In case of multiple cracks, the stress intensity factors can be obtained using the interaction factors presented in Part-I and Newman-Raju solution [Newman Jr.and Raju (1981)]. Here, the interaction factors obtained in Part-I for interacting and coalescing cracks are restated for brevity.

3.1 Empirical Equation for Interacting Cracks

The interaction factors, γ_B, at location φ=180° as given in Table 1 (part-I (Patel et al. [Patel, Dattaguru, Ramachandra(2011)])) are fitted by multivariable least square fit in the following form

$$\begin{aligned}\gamma_B =& a_0 + a_1 \ln(\bar{t}_s) + (a_2 + a_3 \ln(\bar{t}_s)) \left(\frac{a}{c}\right) + (a_4 + a_5 \ln(\bar{t}_s)) \left(\frac{a}{c}\right)^2 \\ &+ (a_6 + a_7 \ln(\bar{t}_s)) \left(\frac{a}{t}\right) + (a_8 + a_9 \ln(\bar{t}_s)) \left(\frac{a}{c}\right)\left(\frac{a}{t}\right)\end{aligned} \tag{7}$$

where $\bar{t}_s$ is normalised interspacing i.e. t_s/c.

The coefficients a_i used in eq. (7) are given in Part-I.

3.2 Empirical Equation for Coalescing Cracks

The interaction factor for coalescing crack at location 'B' is written as

$$\gamma_B = f_{ts} g \left[b_0 + b_1 \left(\frac{a}{c}\right) + b_2 \left(\frac{a}{t}\right) + b_3 \left(\frac{a}{c}\right)\left(\frac{a}{t}\right) + b_4 \left(\frac{a}{c}\right)^2 \left(\frac{a}{t}\right) + b_5 \left(\frac{a}{c}\right)\left(\frac{a}{t}\right)^2 + b_6 \left(\frac{a}{c}\right)^2 \left(\frac{a}{t}\right)^2 \right] \quad (8)$$

where g is a 'fine tune' parameter which should have a limiting values of interaction factor (γ=1) for various aspect ratios and thickness ratios at $\bar{t}_s$=2 (represent single crack) given as

$$g = 1 - 0.12\left(\frac{a}{t} - 0.25\right)(\bar{t}_s)^p \left\{ 1 + 0.3\left(\frac{a}{c}\right)\left(\frac{a}{t}\right) - 0.6\left(\frac{a}{c}\right)^2 \left(\frac{a}{t}\right)^2 \right\}$$

where $p = 1 + \frac{a}{c} + \frac{a}{t}$.

The effect of thickness on the interaction factor is accounted for by the terms in the bracket of eq.(8).

$$f_{ts} = \left(a_0 + a_1 \bar{t}_s^{+} a_2 \bar{t}_s^2 + a_3 \bar{t}_s^3 + a_4 \bar{t}_s^4\right) + \left(a_5 + a_6 \bar{t}_s^{+} a_7 \bar{t}_s^2 + a_8 \bar{t}_s^3 + a_9 \bar{t}_s^4\right)\left(\frac{a}{c}\right) + \left(a_{10} + a_{11} \bar{t}_s^{+} a_{12} \bar{t}_s^2 + a_{13} \bar{t}_s^3 + a_{14} \bar{t}_s^4\right)\left(\frac{a}{c}\right)^2$$

For $\bar{t}_s$<0.1

and

$$f_{ts} = \left(a_{15} + a_{16} \bar{t}_s^{+} a_{17} \bar{t}_s^2\right) + \left(a_{18} + a_{19} \bar{t}_s^{+} a_{20} \bar{t}_s^2\right)\left(\frac{a}{c}\right) + \left(a_{21} + a_{22} \bar{t}_s^{+} a_{23} \bar{t}_s^2\right)\left(\frac{a}{c}\right)^2$$

For $0.1 \leq \bar{t}_s \leq 2$

Where positive and normalised value of interspacing i.e. $\bar{t}_s$ has been considered. The coefficients in eq. (8) are given in Part-I.

4 Experimental Investigation of Surface Crack in Fatigue

Surface crack specimens of aero-engine disk material Inconel-718[Inconel alloy 718 (1985)] are tested at room temperature under uniaxial fatigue loading. Crack

shape development has been investigated in detail. The experimental observations are used in correlating the numerical predictions for fatigue crack growth. Various single and multiple crack shapes have been considered for the investigation. In the numerical simulation, the effect of finite width (for c/W$\geq$0.5) has been taken into account by equation proposed by Patel at el [Patel, Dattaguru, Ramachandra(2005)] and the effect of crack interaction has been taken into account by eqs. (7)-(8).

4.1 Specimen and Material

The surface crack specimens with multiple cracks are considered for testing. The specimen is rectangular in shape in the gauge section having thickness, t, and width, 2W. The major dimensions of the specimen are shown in Fig. 4. The specimen is common in aero-engine industry and is recommended by AGARD committee [Raizenne (1993)].

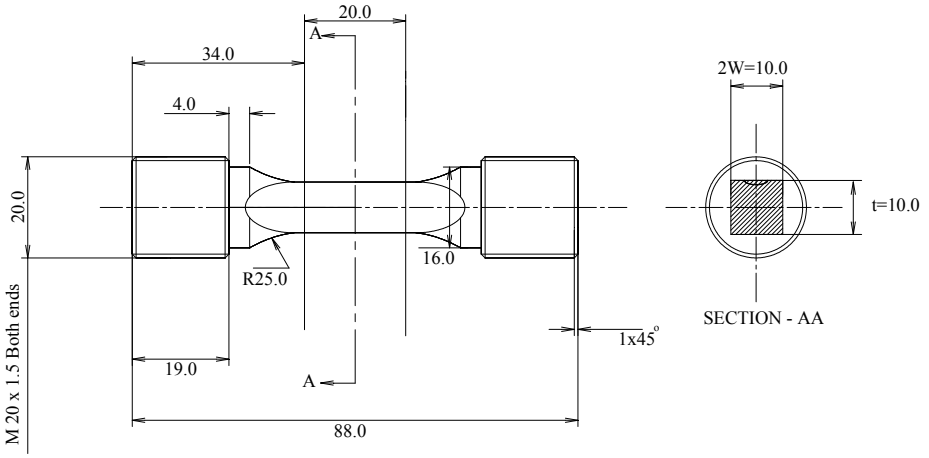

Figure 4: Specimen geometry (dimensions in mm)

The specimen material selected for present study is superalloy Inconel-718 which is extensively used for components of gas turbine engines, liquid rockets, cryogenic tankage etc. Inconel-718 is a high strength, corrosion resistant material used at -252˚C to 705˚F. The specimens are made out of rolled bar of 20mm diameter. The rolled bar was received in hot rolled, solution treated (annealing at high temperature) and machined condition. Subsequently the product was heat treated as

900˚C/1-1/2 hr/AC. The specimens are made using wire cutting EDM (Electrical Discharge Machining). This process usually introduces negligible residual stress in the specimen. The specimens were aged after machining. The ageing heat treatment cycle was 720˚C/8hrs/furnace cooled at 620˚C @ 50˚C/hr/8hrs/Aircooled. The specimens were gradually polished in longitudinal direction (along the loading direction) with emery paper of grade 100 to 600. The specimen was having surface finish of 20 micron.

The material properties are listed in Tab. 1. These material properties were obtained from coupons extracted from the same lot and heat treatment as specimens considered for crack growth study.

Table 1: Mechanical properties of material at room temperature

UTS MPa	0.2 PS MPa	RA %	Hardness BHN	*E MPa	Remark
1470	1210	44	331	29.8E+6	Orientation L

* Nilsson, Harisson, and Mansson (2004)

Various multiple starter flaw shapes are considered as schematically shown in Fig. 5. The initial flaws were created by Electro Discharge Machining (EDM) process. The experimental program covers a wide variety of multiple cracks possible in gas turbine disks.

4.2 Loading Cycle and Frame

All the tests on specimens have been carried out under constant amplitude uniaxial loading. The maximum applied stress was 441.45-674.54 MPa and stress ratio was 0.05. The cycle consists of a loading block, closure detection block and marker blocks. Marker block is used in order to obtain crack shape progression during fatigue testing. The marker block consists of load cycles with the same maximum stress whereas the minimum stress is increased corresponding to stress ratio (R) of value 0.5-0.8. It was observed that the marking block with high stress ratio (R=0.8) gives marking impression of better visibility (or darkness). The loading cycle was triangular in waveform having frequency 2Hz. Although closure cycle block is used during experiments but the processing of closure levels by SEM has not been taken up in this work because it is cumbersome.

The crack growth fatigue test was carried at room temperature in air. The testing was carried out on MTS Servo-Hydraulic Universal Tensile Testing machine. The machine is of variable capacity upto 50T. The load sequences used in experiments were controlled by a micro-console. The machine was calibrated before start of the

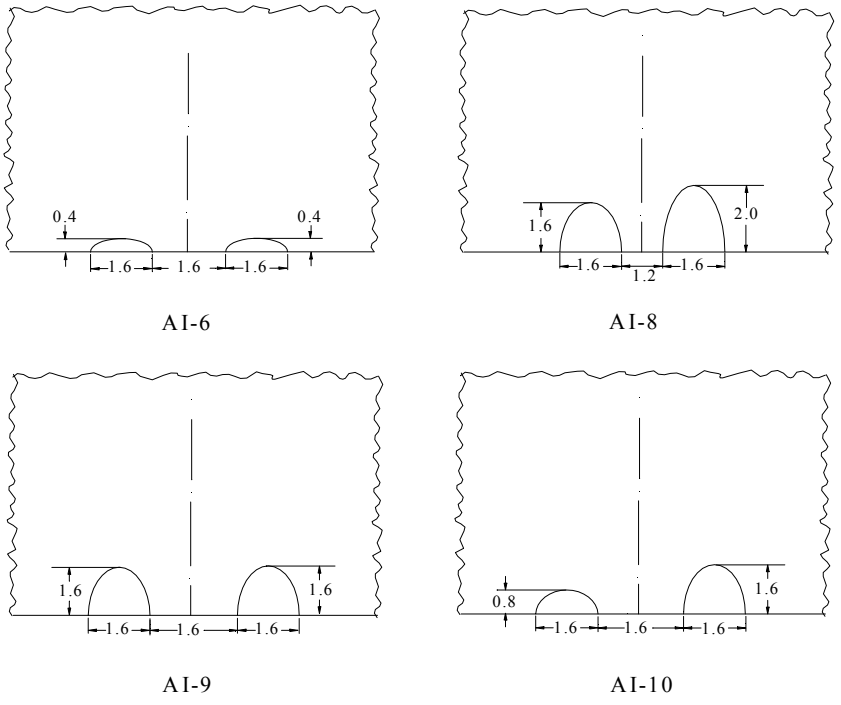

Figure 5: Multiple starters flaw configurations (Schematic)

testing. Also, the accuracy of loading frame was tested on a specimen by measuring strains through a small strain gage mounted on the back face of the specimen. The deviation between experimental and theoretical values is found to be 1.31% at the beginning which reduces to 0.62% at the maximum load. Note that the expected accuracy of strain measuring unit, P3500 [P3500, model SB-10 (1992)], itself is $\pm 3\mu\varepsilon$.

4.3 Experimental and Numerical Studies of Multiple Surface Cracks

The details of crack configurations of multiple cracks (twin semi-elliptical cracks) are given in Tab. 2. The geometry of initial notch is measured from the fracture surface of the specimen. The configurations were tested at stress ratio R=0.05. Similar to single crack, the benchmarks were created by changing the minimum load during the fatigue testing of the specimens. The photographs of fracture surface of specimens are shown in Fig. 6(a)-(d). The experimental results and the numerical

simulation are discussed in the following sections:

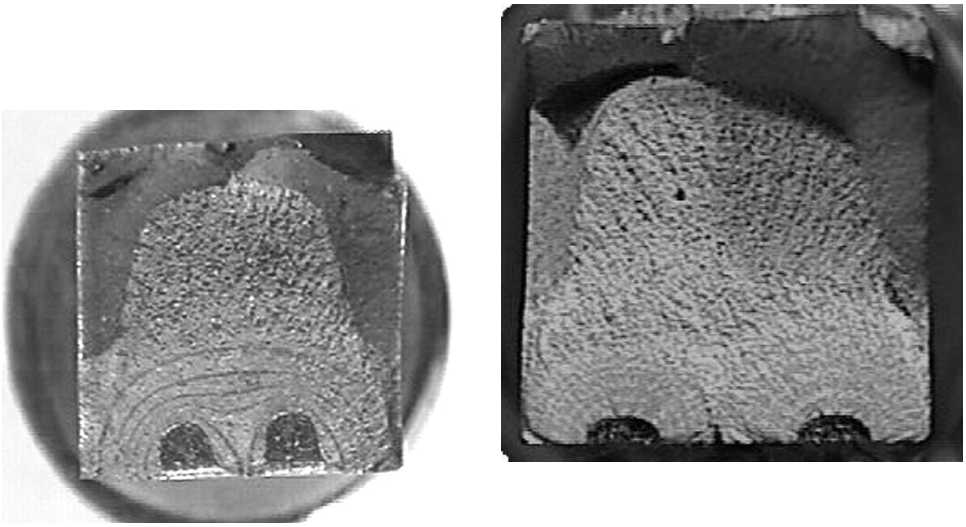

(a) (b)

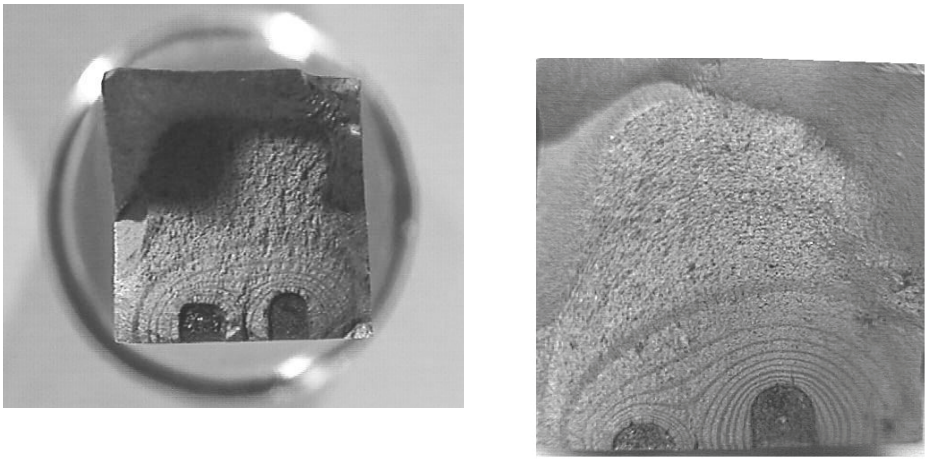

(c) (d)

Figure 6: (a) A digital photograph of fracture surface of specimen AI-9. (b) A digital photograph of fracture surface of specimen AI-6. (c) A digital photograph of fracture surface of specimen AI-8. (d) A digital photograph of fracture surface of specimen AI-10

Table 2: Details of multiple surface cracks test configurations

Description	**ID**	**Crack 1 a_0 c_0 (mm)**		**Crack 2 a_0 c_0 (mm)**		**t_s t_s/c***	**σ_{max} (MPa)**	**R for loading cycle**	**R for marker cycle**
Equal# and deep	AI-9	1.6623	0.8523	1.7045	0.8717	0.8026 0.942	674.54	0.05	0.8
Equal# and shallow	AI-6	0.6648	0.9282	0.6597	0.9491	1.5777 1.699	674.54	0.05	0.5
Unequal and deep	AI-8	1.6575	1.0231	2.0176	1.0066	0.5932 0.5845	674.54	0.05	0.8
Highly unequal	AI-10	0.619	0.752	1.556	0.907	0.9213 1.1107	674.54	0.05	0.8

Assumed to be equal, though the cracks are marginally different in size.

*In case of unequal cracks 'c' is defined as an average of two cracks.

4.3.1 Deep and Equal Twin Semi-Elliptical Cracks

The measured points on crack fronts are shown in Fig. 7. The points on each front are fitted by an ellipse using least square fit technique. The points near the free surface are not considered in curve fitting. It is observed that during coalescence the crack front fits well into elliptical shape if the shift in the center of ellipse is considered. After the coalescence of cracks, the single crack is found to have less curvature at center whereas higher curvature near the free surface compared to an ellipse, still it can be reasonably represented by an elliptical shape.

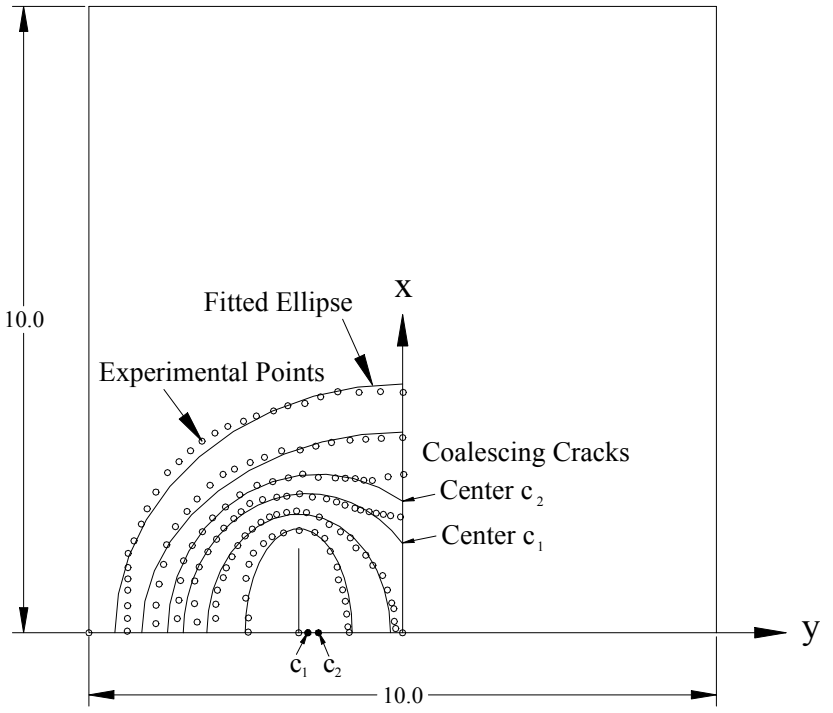

Figure 7: Measured points on the crack front and fitted ellipse

The crack shape development (aspect ratio v/s thickness ratio) obtained from experiment is compared with numerical prediction in Fig. 8. The numerical predictions are carried out using model presented in the previous section. The predictions were also made considering crack closure. Numerical predictions are found to be in

good agreement with experimental results in interaction phase. Higher deviations in numerical predictions are observed in the crack coalescence phase. In this phase, the model with closure predicts 24.9% higher aspect ratio whereas model without closure predicts 29.9% higher aspect ratio at a/t=0.216. This is principally due to uncertainty involved in transition from interaction and coalescence phase, and secondly due to effect of crack curvature at coalescence region. In the prediction model the transition from interaction and coalescence phase is assumed to be gradual and elastic whereas in reality the cracks suddenly form the coalescence due to failure of plastic ligament between cracks. This is observed in three-dimensional cracks by Soboyejo et al. [Soboyejo, Knott, Walse and Cropper (1990)]. Secondly, the concave curvature of cracks at the coalescing plane is expected to reduce the interaction factor. In the absence of advance information on crack curvature and its variation with crack growth at coalescence plane it is difficult to consider it in analysis and thus not included in estimation of interaction factor. In fact, the present approach neglecting the curvature keeps the simplicity of both the crack growth model and the coalescence analysis.

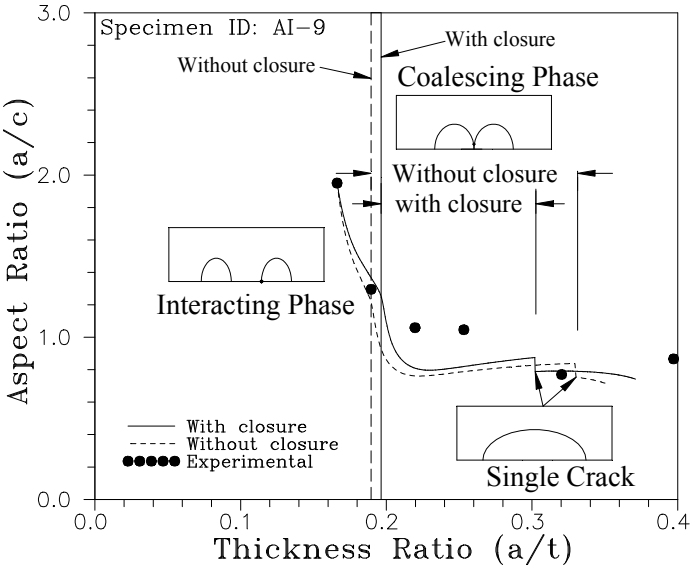

Figure 8: Crack shape development for twin deep interacting semi-elliptical cracks in fatigue

The model including closure predicts smaller coalescence region relative to model neglecting closure phenomenon. The model including closure predicts the beginning of coalescence phase at a/t=0.196 whereas the model neglecting closure predicts the beginning of coalescence phase at a/t=0.189. The higher closure levels at the surface (U_C/U_A=0.9158) leads to slower crack growth at location 'C' relative to model excluding closure. Thus, the model considering crack closure predicts the beginning of coalescence phase at higher thickness ratio. The closure effects also lead to higher aspect ratio for the same thickness ratio as observed in study of single crack. Since the interaction factor increases with aspect ratio the model with closure phenomenon predicts early completion of coalescence region.

Figure 9 shows the variation of interaction factor during crack progression. The crack growth starts with positive t_s/c i.e. from right side of the graph marked by an arrow. Interaction was not observed till t_s/c is approximately equal to 0.4 after that interaction factor increases and reaches to maximum value of 1.88. The interaction factor increases to 4.64 at the beginning of coalescence phase but drops very rapidly and subsequently it decreases and reaches an asymptotic value close to one.

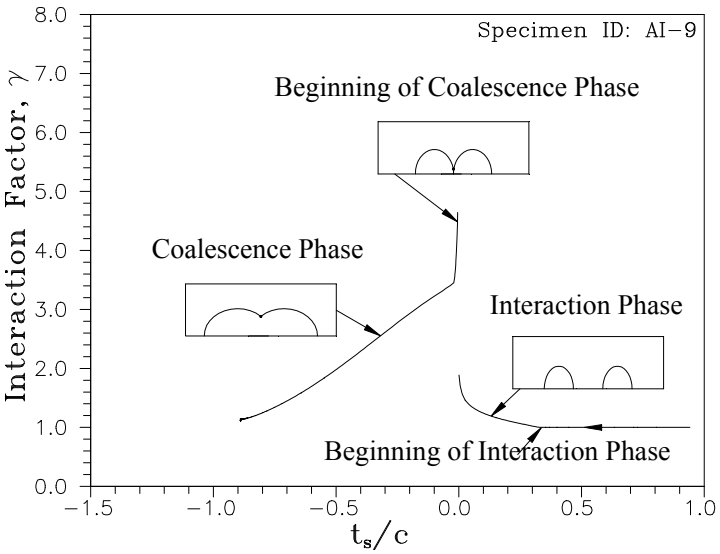

Figure 9: Variation of interaction factor during various stages of fatigue crack growth of twin semi-elliptical cracks

The experimental life with crack lengths 'a' and 'c' is compared with predictions in

Fig. 10. The numerical model predicts a higher growth rate in c-direction in coalescence region. The coalescence phase consumed more than 25% of total propagation life. The predicted life is found to be 3.4% higher relative to experimental life of this specimen.

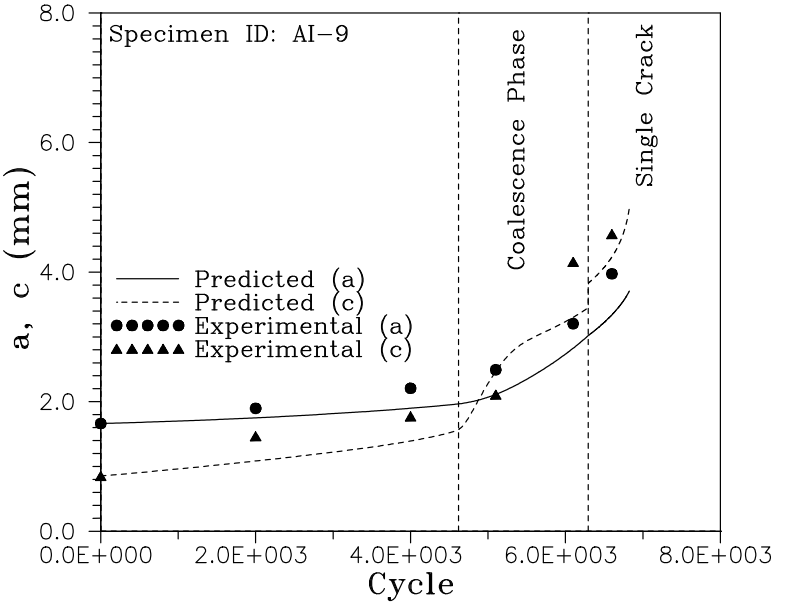

Figure 10: Experimental and predicted life for specimen AI-9

4.3.2 Equal and shallow twin semi-elliptical cracks

The measured points on the crack fronts are shown in Fig. 11. The points on each front are fitted by an ellipse using least square fit technique. Only one front could be captured during crack growth in the coalescence phase. This front shape is typical near the completion of coalescence phase as observed in the first specimen (AI-9) where the crack front has less curvature at center and higher curvature near the free surface compared to the fitted ellipse. Here, the crack front is further truncated as it crosses the side faces of the specimen.

The crack shape development (aspect ratio v/s thickness ratio) obtained by experiments are compared with numerical predictions in Fig. 12. Both numerical and experimental results show increase in aspect ratio as cracks grow similar to a single

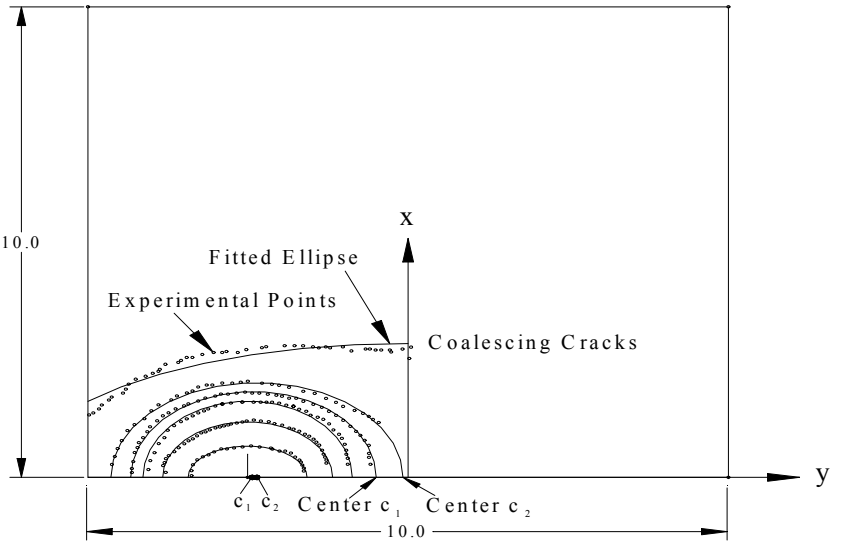

Figure 11: Measured points on the crack front and fitted ellipse

crack. Subsequently, the cracks grow faster in 'c' direction as they come in close vicinity (t_s/c<0.5) due to interaction effects. This is also evident from the experimentally obtained crack front as shown in Fig.11, the tips of the cracks towards the center grow faster as compared to the tips of the cracks at outer sides. This also leads to a slight shift in the center of crack (center of semi-ellipse). During interaction phase the interaction factor reaches a value 1.67 (Fig. 13).

It is difficult to obtain a beachmark exactly at the beginning of the crack coalescence experimentally, thus a beachmark (a/t=0.201) just before the coalescence is taken approximately as the beginning of coalescence phase in fatigue crack growth of multiple cracks. Using this, it is observed that the model without closure predicts crack coalescence early (a/t=0.197) whereas the model with closure predicts late crack coalescence at a/t=0.217. The numerical models predict sudden drop in aspect ratio during initial stage of coalescence phase. This is due to higher interaction factor at the beginning of coalescence phase as shown in Fig 13. The predictions are made only upto crack growth c/W=1.0 i.e. the crack tips just touch the side faces of the specimen thus the last experimental data point could not be simulated.

The experimental life with crack lengths 'a' and 'c' is compared with predictions in

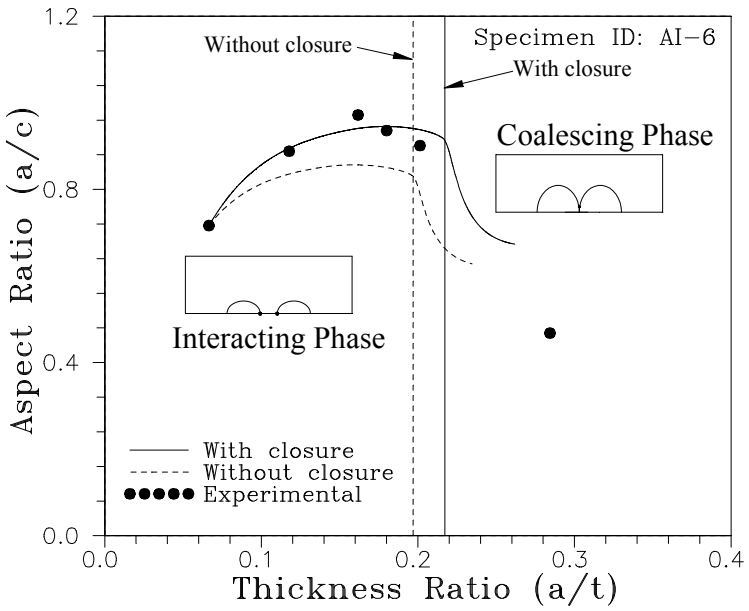

Figure 12: Crack shape development for twin shallow equal interacting semi-elliptical cracks in fatigue

Fig. 14. Also, for this specimen the numerical model predicts a higher growth rate in c-direction in coalescence region. The life spent in coalescence phase is found to be insignificant (4.08% of total propagation life). This is due to large initial spacing between the cracks. By the time the cracks coalescence the crack growth rate would be very high since it would be dictated by the upper region of crack growth rate curve (da/dN v/s ΔK) and therefore life spent in the coalescence phase would be insignificant. The prediction model overestimates life by 15.9%.

4.3.3 Unequal and Deep Twin Semi-Elliptical Cracks

This configuration (AI-8) has two unequal inplane cracks separated by a distance 1.186mm. The geometries of the cracks are as follows:
LHS Crack: a_o/t=0.1657, a_o/c_o=1.62 and
RHS Crack: a_o/t=0.2017, a_o/c_o=2.00

The measured points on crack fronts are shown in Fig. 15. The figure also shows the corresponding ellipses obtained by least square fit of points on each front. It is noted that the centers of the cracks move inward (towards the coalescence plane). The shift in crack center increases as coalescence progresses. This is also included

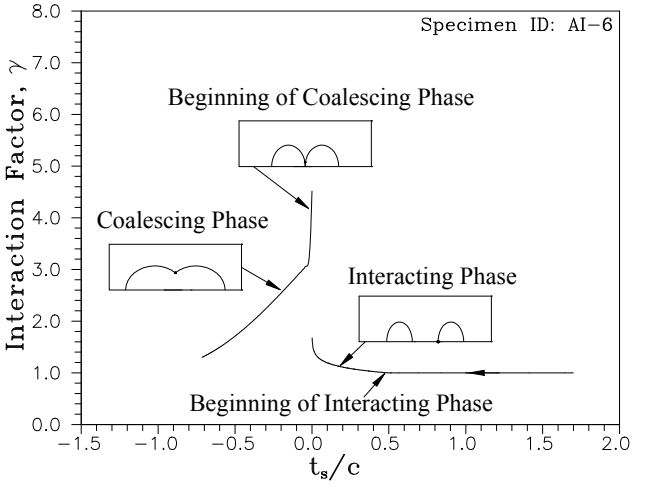

Figure 13: Variation of interaction factor during fatigue crack growth of twin shallow semi-elliptical cracks

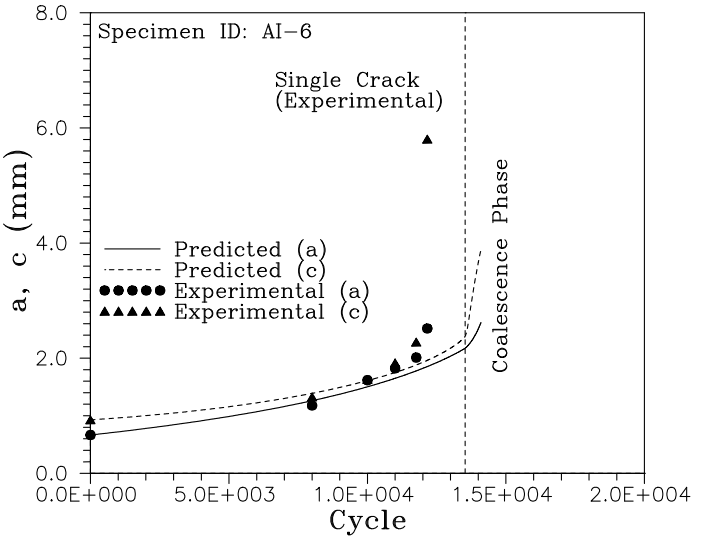

Figure 14: Experimental and predicted life for specimen AI-6

during the least square fit of points to an ellipse. It is observed that the semi-ellipse with shifted center represents the crack front accurately till the formation of single crack. It could be seen from Fig. 15 that the smaller crack grows faster such that at the end of coalescence its geometry is nearly equal to the bigger crack. The single crack at the end of coalescence could be represented by an ellipse in an approximate way.

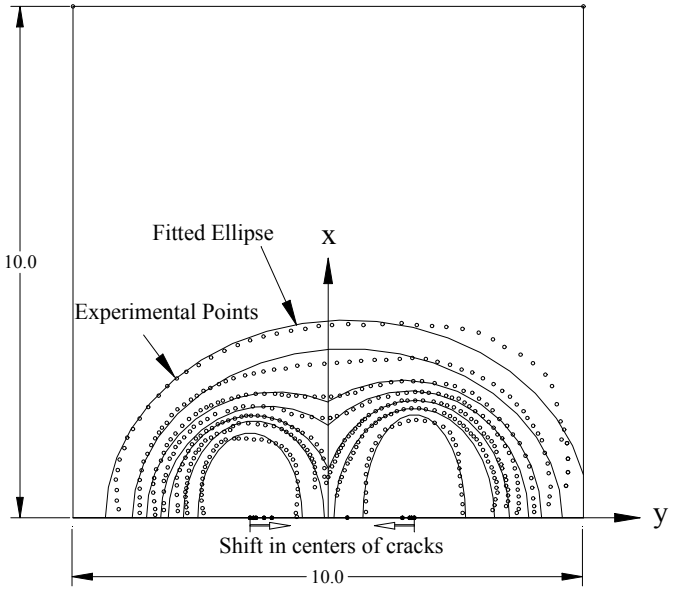

Figure 15: Measured points on the crack front and fitted ellipse

Figure 16 shows the predicted and experimental crack shape development. The shift in the crack centers is included in the crack growth model. The effect of crack closure is considered in the prediction model. Although the interaction factors eq. (7) and (8) are applicable for symmetric cracks, the interaction factor equations are used for unsymmetric surface cracks as well. During the interaction phase, the interaction factors are evaluated based on the geometry of individual crack assuming that the cracks are symmetric. However, during the coalescence of cracks the interaction factor is evaluated based on average geometry of the cracks since the interaction factor would have to be the same for both the cracks in this phase. The predicted crack coalescence starts at a/t=0.1965 and 0.2214 and corresponding experimental values are 0.189-0.20 and 0.214-0.2308 for left and right hand side

cracks respectively. This shows that the fatigue crack growth of twin interacting cracks can be predicted accurately by the proposed crack growth model. The experimental values are given in a band since it is not possible to obtain a benchmark exactly at the starting of the coalescence phase.

Experimental and numerical studies show that there exists a preferred propagation path for multiple cracks as both cracks start propagating with different initial aspect ratios but at the end of the coalescence they reach almost the same aspect ratio. The predictions in the coalescence region represent the trend of crack growth accurately except at the beginning of coalescence phase where numerical model predicts a rapid drop in the aspect ratio of the crack. At this point in time during fatigue (a/t=0.2183), the numerically predicted aspect ratio is found to be 22.9% lower than the experimental value. The cracks are assumed to form a single crack at end of coalescence phase which is predicted to be at a/t=0.2986. The completion of end of coalescence phase is assumed to occur at y_{coal}/a=0.99. In this region the numerically predicted crack shape development compares well with experimental values.

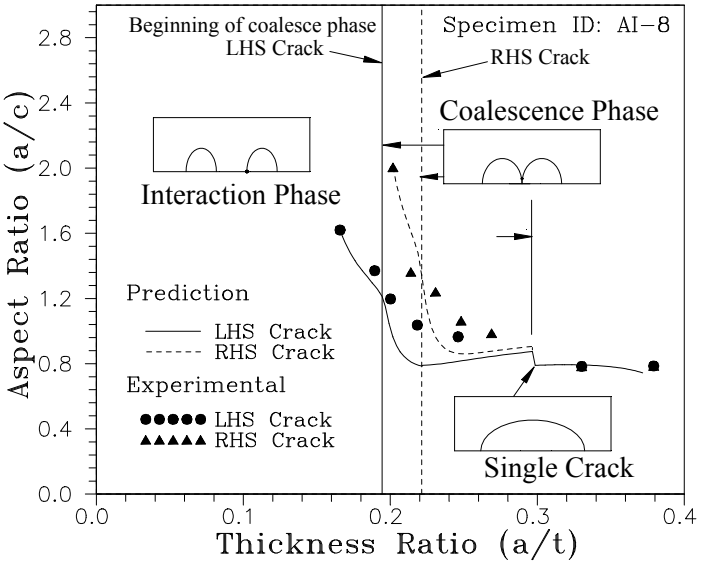

Figure 16: Experimental and predicted crack shape development for twin unequal semi-elliptical cracks

The experimental life for left crack is compared with numerical prediction in Fig. 17. The predicted life compares well with experimental life in the interaction phase. At N=3000, in the interaction phase, the numerically predicted 'a' and 'c' are found to be 0.3% lower and 7.2% higher compared to experimental values. The coalescence phase consumes 32.92% of the total propagation life. Although, the propagation life of this configuration is found to be the same as that obtained from experiment, this is mere coincidence since predicted life in the interaction phase is shorter while in the coalescence phase it is longer as compared to experimental values.

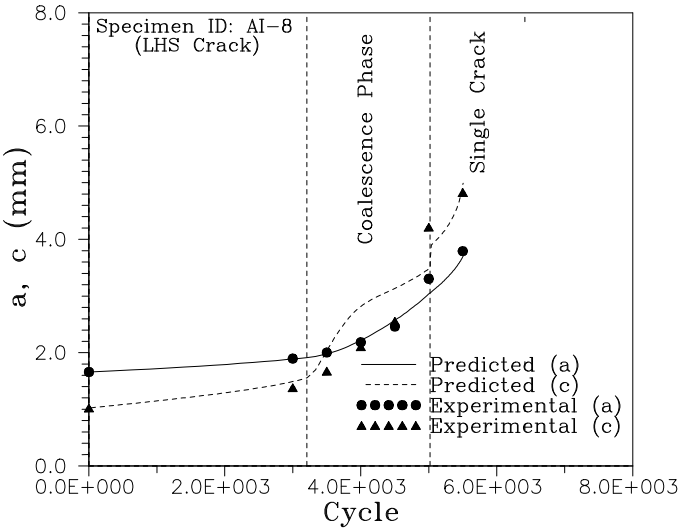

Figure 17: Experimental and predicted life for specimen AI-8

4.3.4 Highly Unequal Twin Semi-Elliptical Cracks

This configuration (AI-10) has been considered to study the effect of a small semi-elliptical crack on a larger semi-elliptical crack. The geometries of the cracks are as follows:
LHS Crack: a_o/t=0.0619, a_o/c_o=0.823 and
RHS Crack: a_o/t=0.1556, a_o/c_o=1.716

The measured points on the crack fronts are shown in Fig. 18. The figure also shows the corresponding ellipses obtained by least square fit of points on each front. It is noted that the center of smaller crack shifts inside (towards the other crack) faster relative to the center of the larger crack. The shift is indicator of unequal crack

growths at locations 'B' and 'C'. Due to effect of interaction between two cracks the growth at location 'B' will be higher than that at 'C'. Thus higher shift in the center of smaller crack shows that smaller crack experiences higher interaction effect compared to larger crack. Although, there was large difference in the initial shapes of the cracks, the crack fronts maintain the shapes close to semi-ellipse.

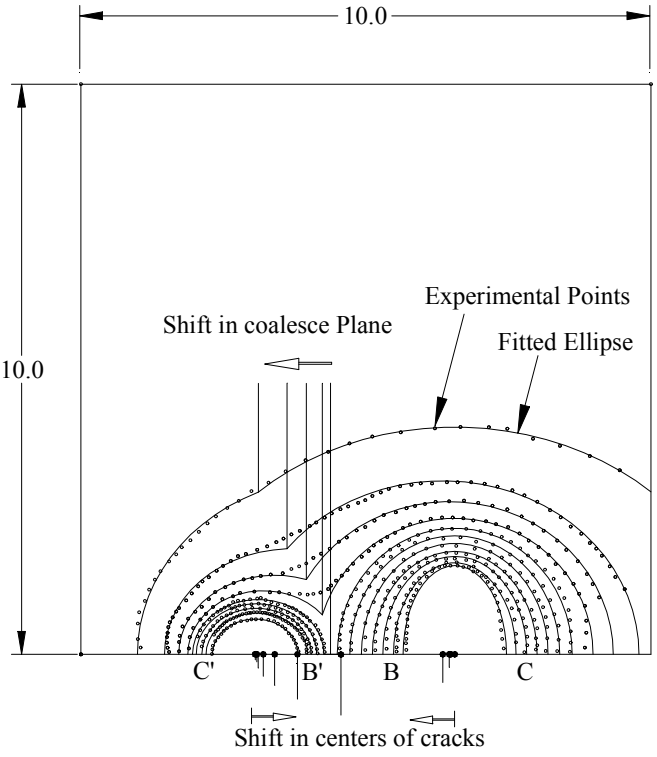

Figure 18: Measured points on the crack front and fitted ellipse

Fig. 19 shows the predicted and experimental crack shape development. The experimental results show that the smaller crack nearly maintains the same aspect ratio throughout the crack growth. Although the interaction factor eqs. (7) and (8) are applicable for symmetric cracks, the interaction factor equations are used for nonsymmetric surface cracks as well. The predicted crack coalescence starts at a/t=0.099 and 0.234 and corresponding experimental values are 0.096-0.111 and 0.221-0.238 for smaller (LHS) and larger (RHS) cracks respectively, which shows that the model predicts the beginning of coalescence accurately. The aspect ratio

of larger crack is predicted accurately but for the smaller crack the aspect ratio is found to be 9.17% higher just before the coalescence relative to the experimental value. This may be due to lower interaction factor as estimated under the assumption of symmetric cracks. It is expected that if a small crack exists in the vicinity of relatively larger crack, the interaction factor would be higher. Also, it is assumed that the coalescence plane remains at the same location throughout the crack growth but the experimental results clearly show that coalescence plane in fact translates towards the smaller crack.

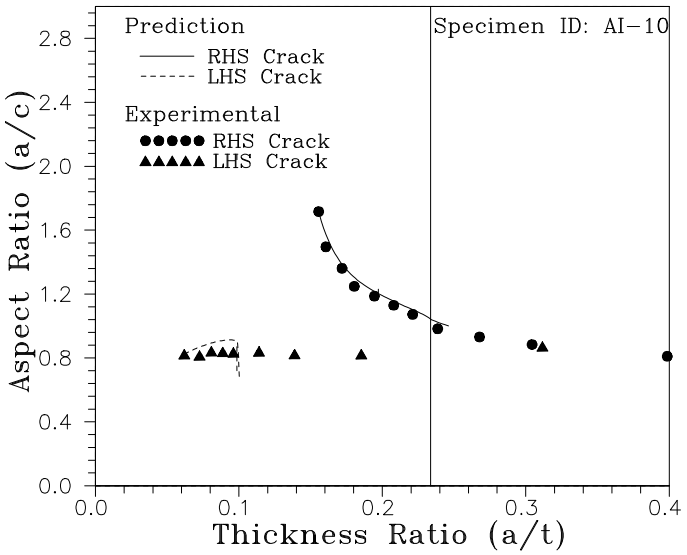

Figure 19: Crack shape development for twin unequal semi-elliptical cracks

The experimental life for left crack is compared with the numerical prediction in Fig.20. The crack prediction is stopped as surface crack length of larger crack, 'c' tends to 'W' (c→W) whereas the experimental life is given upto the last crack front. Thus the experimental and predicted life is compared at the same crack depth. At crack depth (a/t=0.238), the predicted life is found to be 18% higher relative to the experimental life. The coalescence phase consumes 23.33% of total propagation life as shown by the experimental results.

Although, the crack growth model for multiple cracks predicts the crack shape and life in the presence of two unequal cracks to a reasonable accuracy, further improvement can be made if empirical interaction factor equations for unequal cracks are made available and used in the model. The model can also be improved to account for the shift in the coalesce plane as observed for this configuration.

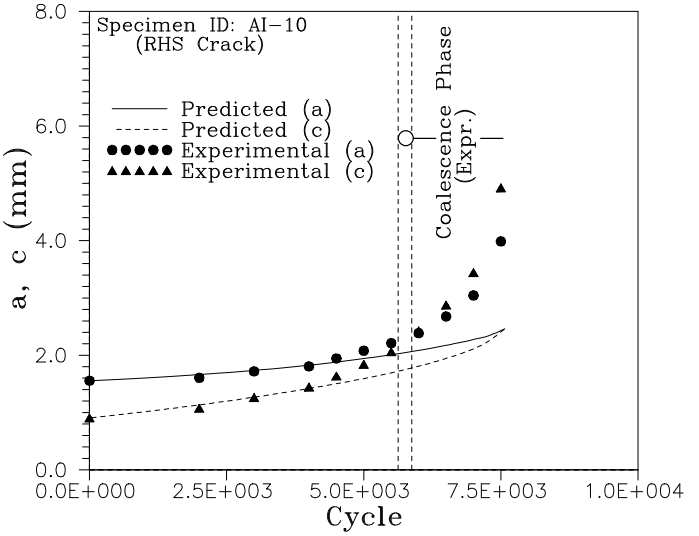

Figure 20: Experimental and predicted life for larger crack

5 Concluding Remarks

Using the interaction factors for twin coplanar semi-elliptical cracks, empirical equations are formulated for interacting and coalescing cracks to facilitate their direct use in the fatigue crack growth simulation of multiple cracks.

Experiments were also conducted to study the effects of multiple cracks on crack shape development and propagation life. It is observed that the centers of cracks shift towards the coalescence plane during the fatigue growth of the cracks. It is found that similar to a single crack the crack fronts in the presence of multiple cracks can be approximated by part-ellipses if the shift in the centers of cracks is taken into account. It is found from experimental study that in case of relatively large crack in the neighbourhood of a small crack coalescence plane also shifts. The life spent in the coalescence phase is found to be as high as 33% of the total propagation life of the specimen, thus it should not be ignored, particularly in life limiting structures such as aircraft and aero-engines.

Three degrees of freedom crack growth model for estimation of crack shape development and life of multiple cracks has been proposed. The model was verified using the experimental results. The model is found to be accurate for prediction of crack shape during interaction phase. However, the model underestimates the aspect ratio during coalescence phase. Predictions in coalescence phase can further be improved by consideration of the effect of curvature of cracks at coalesce

plane. In the case of largely different shaped cracks (case-4, specimen ID: AI-10), the model could be improved by taking into account the shift of crack coalescence plane.

The proposed three degrees of freedom model for interacting and coalescing cracks is found to predict the crack propagation life accurately. The predicted lives for the considered four configurations are found to be higher by 3-18% compared to experimental lives.

In general, it is clear from the present study that the life of surface cracks, single or multiple, can be predicted accurately if the stress intensity solutions, interaction factors and crack closure factors are available for the configurations and the material.

References

ASTM E740 (1987): Metal test methods and Analytical Procedures, *Annual Book of ASTM Standards*, vol. 03, no. 1, pp. 941.

BSI PD6493 (1980): Guidance on some methods for the deviation of acceptance levels for defects in fusion welded joints, British Standards Institution, *BSI PD6493, Section 3*.

Grandt, Jr. A. E. (1986): An experimental and numerical investigation of the growth and coalescence of multiple fatigue cracks at notches, *ASTM STP 905*, pp. 239-252.

Iida, K. (1983): Shapes and coalescence of surface fatigue cracks, *Proc. of ICF International Symposium on Fracture Mechanics, Beijing, China*, pp. 679-693.

McComb, T. H.; Pope, J. E.; Grandt, Jr. A. F. (1986): Growth and coalescence of multiple fatigue cracks in polycarbonate test specimens, *Engng. Fract. Mech.*, vol. 24, pp. 610-608.

Newman, Jr. J. C.; Raju, I. S. (1981): An empirical stress intensity factor equation for the surface flaw, *Engng. Fract. Mech.*, vol. 15, pp. 185-192.

Nilsson, F.; Harisson, T.; Mansson, T. (2004): Growth of surface Cracks under constant and variable amplitude loading, *Engng. Fract. Mech.*, vol. 71, pp. 1725-1735.

P3500, model SB-10 (1992): Portable strain indicator, Instruments Div., *Measurements group, Inc., Raleigh.*

Patel, S. K.; Dattaguru, B.; Ramachandra, K. (2005): Experimental and numerical prediction of surface crack growth in fatigue in a finite width plate, *J. of Aerospace Sciences and Technologies*, Vol. 57, No. 1 , pp. 323-331.

Patel, S. K.; Dattaguru, B.; Ramachandra, K. (2011): Multiple interacting and

coalescing semi-elliptical surface cracks in fatigue- Part-I: Finite element analysis, *SL: Structural Longevity*, Vol. 36, No. 1 , pp. 1-21.

Raizenne, M. D. (1993): Fatigue crack growth results for Ti-6Al-4V, IMI685 and Ti-17, AGARD Engngine Disc Cooperative Test Program, *AGARD R-766 (Addendum).*

Soboyejo, W. O.; Knott, J. F.; Walse, M. J.; Cropper, K. R. (1990): Fatigue crack-propagation of coplanar semi-elliptical cracks in pure bending, *Engng. Fract. Mech.*, vol. 37, pp. 323-340.

Soboyejo, W. O.; Kishimoto, K.; Smith, R. A.; Knott, J. F. (1989): A study of the interaction and coalescence of two coplanar fatigue cracks in bending, *Fat. Fract. Engng. Mater. Struct.*, vol. 12, pp. 167-174.

Song, P. S.; Shen, B. C.; Shieh, Y. L. (2002): Predicion of semi-elliptical surface crack growth in 2024-T4aluminum alloy, *Int. J. Pressure vessel and piping*, vol. 79, pp. 273-278.

Song, P. S; Sheih, Y. I.(2004): Crack growth and closure behavior of surface cracks, *Int. J. Fatigue*, vol. 26, pp. 429-436.

To, S.; Lambert, S. B.; Burns, D. J. (1993): A multiple crack model for fatigue in welded-joints, *Int. J. Fat.*, vol. 15, pp. 333-340.